A Comparative Examination of the Structural and Physicochemical Characteristics between Algeria Valleys and Dunes Sand

E. Bekkar[1], S. Benchaa[1], A. Achouri[2], M. Touil[2], MSE. Bougoffa[3], R. Gheriani[1*], H. Belkhalfa[4]

[1] Univ Ouargla, Fac. Mathematics and Material Sciences, Lab. Radiation and Plasmas and Surface Physics Laboratory (LRPPS), Ouargla 30000, Algeria.

[2]Univ Ouargla, Fac. Mathematics and Material Sciences, Lab. Development of Renewable Energies in Arid and Saharan Zones, Ouargla, 30000 Alegria.

[3]Univ Houari Boumediene, Fac. Science and Technology, Lab. Materials Technology, Houari Boumediene, Bp 32 El Alia, Bab Ezzouar, 16111, Algeria.

[4]Univ Ouargla, Scienifc and Technical Reserch Center in Physico-Chemical Analysis (CRAPC), Ouargla, Algeria.

Email: ragheriani@yahoo.fr

Received: 25/05/2023; Accepted: 26/11/2023; Published : 12/12/2023

Abstract

This study explores the physical, chemical, and microstructural attributes of two different types of natural sand , specifically white sand and dune sand from Bir El Ater river in the north east and Engoussa in the southeast of Algeria. Various analytical methods have been used such as Fourier-transform infrared (FTIR) spectroscopy, X-ray diffraction (XRD), X-ray Fluorescence (XRF), Scanning electron microscopy (SEM) and laser dispersion particle size. The FTIR and XRD analyses confirm that both white sand and dune sand are primarily composed of high proportions of α-quartz (SiO_2), while containing minimal quantities of calcite ($CaCO_3$) and gypsum minerals ($CaSO_4$;$2H_2O$). The chemical analysis further confirms that both sand types exhibit significant silica (SiO_2) content, its percentage of white sand is 92.95% and 44.63% of dune sand, alongside very low amounts of Al_2O_3, Fe_2O_3, K_2O and Na_2O oxides. The dune sand had a greater CaO content compared to the white sand. The grain samples of the white sand have shapes ranged from sub-angular, rounded, surrounded, well-rounded and irregular. In contrast, the dune sands featured shapes that ranged from sub-angular to well-rounded. For Bir El Ater samples, the values are between 51.471 and 1754.613 µm, while for Engoussa samples, the values are between 200 to 3019.738µm.

These results indicate that both white sand and dune sands exhibit mineralogical stability and possess suitable chemical properties for application as fine aggregates in construction. Moreover, these sands have the potential to serve as valuable sources of quartz minerals. The findings from this study provide valuable insights for identifying specific industrial and nanotechnology applications for each of these sand types.

Keywords: Sand, XRF, XRD, FT-IR, Particle size, SEM, Algeria.

Tob Regul Sci.™ 2023;9(2): 2075 - 2086

DOI: doi.org/10.18001/TRS.9.2.134

1. Introduction

The significant expansion of industry and infrastructure has led to heightened demand for construction materials, specifically natural sand, across a range of applications. River sand reserves are notably limited in various regions, especially deserts. For this reason, there's a compelling need to explore alternative sources of high-quality materials for construction projects, with a primary focus on optimizing the use of local resources [1].

The appeal of dune sand as a construction material lies in its characteristics and low cost, especially in arid areas where fine natural aggregates are scarce, while dune sands are abundantly available [2].

In accordance with most building material recommendations and standards, dune sand is a potentially suitable option due to its typically well-balanced particle size distribution and robust resistance to water [3]. Fine aggregate constitutes roughly one-third of the total concrete aggregates and plays a crucial role in filling gaps [4]. Moreover, fine aggregates are essential for maintaining the smoothness and cohesion of concrete [5]. Dune sands are unconsolidated sediments that form through the wind-driven erosion, transportation, and deposition of weathered materials from a sandy parent source in arid environments [6]. They possess distinct granular properties characterized by their highly uniform particle size distribution, fine average size, rounded particle shapes, and the challenge of achieving proper compaction without adequate lateral confinement [7].

Recently, there has been a growing focus on utilizing aeolian sands as a construction material in applications such as concrete, mortar, and pavement. In a study conducted by Amri et al. (2019)[8], the impact of dune sand treatment on the geotechnical, structural, and mineralogical properties of clayey soil was explored. Their findings demonstrated a significant enhancement in the geotechnical characteristics when dune sand was introduced to the clay. According to Moulay-Ali et al. (2021)[9], the optimal blend of 20% dune sand, 40% quarry sand, and 60% crushed sand offers superior mechanical strength in terms of concrete compression. Luo et al. (2013)[10] discovered that concrete containing extremely fine dune sand grains from the Australian desert exhibited workability and durability comparable to concrete made with river sand. In another study by Smaida et al. (2019) [11], it was revealed that dune sand, when processed with cement, pozzolan, and limestone, saw improvements in its mechanical properties, making it suitable for use in pavement foundation layers. Hence, there is a critical need to investigate the physicochemical characteristics of dune sand to determine its suitability for construction applications.

Algeria stands as the largest country in Africa, boasting extensive stretches of sand dunes that envelop approximately one-quarter of its landmass. The Algerian Sahara contains one of the largest eolian dune deposits in the world (approximately 2.4.106 km2) [12]. These sand dunes are

categorized into "ergs," which are vast expanses of continuous sand dunes, i.e., large areas of continuous dunes, of which the Grand Oriental Erg is the most important [13].

It can be defined as a granular material consisting of small grains of different sizes as a result of the decomposition of materials of mineral or organic origin such as rocks, shells, coral and skeletons. Its diameter ranges from 0.063 as silt to 2 mm gravel. Its composition can reveal up to 180 different minerals quartz, micaand feldspar as well as limestone remnants. Sand takes its colours from its components, range from bright red to black [14-15].

To determine whether Engoussa dune sand is suitable for construction, a comprehensive examination of its physicochemical properties is essential. This study conducts a detailed investigation into two sand varieties, providing a thorough comparative analysis of their physical characteristics. It includes non-destructive chemical assessment techniques like X-ray fluorescence (XRF) and Fourier-transform infrared spectroscopy (FTIR), mineralogical analysis using X-ray diffraction (XRD), and morphological evaluation through Scanning Electron Microscopy (SEM).

2. Experimental

2.1. Materials and Methods

Our study focuses on two specific regions within Algeria: the Engoussa region in the Ouargla province, located in the southeastern portion of the Algerian desert, and Bir El Ater in the Tebessa region, situated in the eastern part of the Algerian Sahara. We have provided the geographical coordinates for these regions: Ouargla [31° 57'N, 5° 18'E] and Bir El Ater [34° 44' 55" N, 8° 03' 29" E]. The positions of these two regions are clearly marked on the Algerian map depicted in Fig. 1.

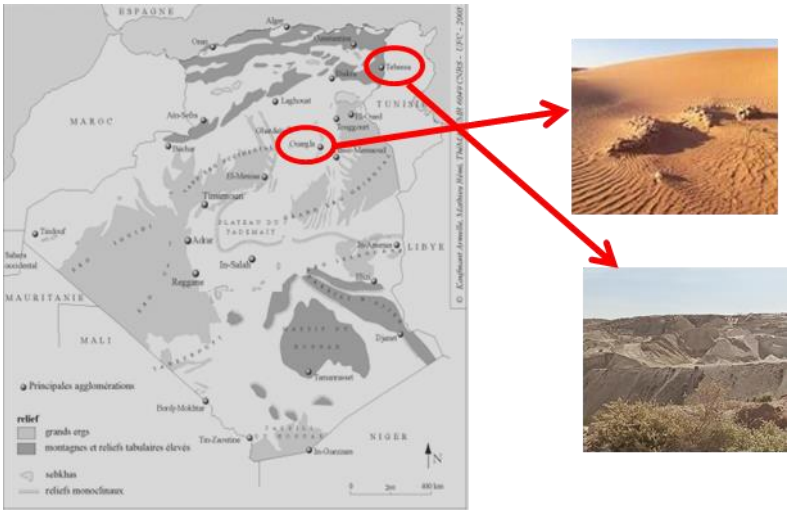

Fig. 1. Locations of the collected sand samples [15].

The sand samples (Fig. 2) under investigation were collected from various depths and diverse locations. To prepare them for XRD and FTIR analysis, the samples were effectively pulverized using a pottery mortar, after which they were stored in airtight plastic containers at ambient room temperature.

Fig. 2. The studied samples before preparation: the white sand (S1), Dune sand (S2).

2.1.1. X-ray Fluorescence (XRF)

The analysis of the samples' chemical composition was conducted using a non destructive, rapid, and multi-elemental technique known as X-ray Fluorescence (XRF). In this method, the samples were exposed to a primary x-ray beam, causing the material to emit specific x-ray lines that enable the identification of its chemical elements and their respective atomic or mass concentrations. In this measurement, the powdered sample was combined with a small quantity of triethanolamine ($C_6H_{15}NO_3$). The resulting mixture was then subjected to high pressure

for a few minutes to create a pellet for measurement.

2.1.2. X-ray Diffraction method (XRD)

X-ray diffraction (XRD) was utilized to semi-quantitatively identify chemical phases. The analysis was carried out using a Philips X'Pert PWR X-ray diffractometer equipped with a Cu-tube (λ = 1.5406 Å), operating at an accelerating voltage of 40 kV and a current of 30 mA. The measurements involved scanning 2θ angles ranging from 10 to 60° with a step size of 0.02 degrees per second (degrees/sec).

2.1.3. Fourier transformation infrared spectroscopy method (FTIR)

To analyze the molecular vibration bonds present in our samples, a Thermo Scientific Nicolet 380 FT-IR spectrometer was employed, covering the spectral range from 400 to 4000 cm^{-1}. The sample preparation involved combining 1 mg of sand with 100 mg of dry potassium bromide. This mixture was subsequently compressed to create a pellet with a 13 mm diameter.

2.1.4. SEM morphological analysis and Grain size distribution

The evaluation of the morphological aspect of the studied samples was conducted using a Scanning Electron Microscope (SEM) from Carl Zeiss Microscopy GmbH in Jena, Germany. Additionally, the grain size distribution of the samples in their natural state was determined through the employment of the laser diffraction technique using the LA-960 HORIBA instrument.

3. Results and Discussions

3.1. X-ray Fluorescence (XRF)

Table 1 displays the chemical compositions of the sand samples study by WDXRF analysis. It should be noted that the sand samples all exhibit elevated silica contents (SiO_2) ranging from 92.95% to 88.03%, accompanied by minimal levels of calcium oxide (CaO). Notably, the white sand sample (S1) demonstrates the highest silica content (92.05%) and the lowest calcium oxide percentage (2.27%). Conversely, the dune sand sample (S2) presents the lowest silica content (88.03%) and higher levels of calcium oxides (8.89%). Additionally, trace amounts of Al_2O_3, Fe_2O_3, and K_2O were observed in all samples.

The S1 sample revealed an alumina content of 2.77%, with concentrations of Fe_2O_3 and K_2O varying between of 0.36% to 2.14% and 0.34% to 0.42% respectively. Some other trace oxides, such as MgO and Na_2O were detected.

As a result, the elevated silica content found in the examined sand samples validates their siliceous nature. Nonetheless, the presence of minor impurities, specifically Al_2O_3, CaO and MgO could potentially influence the technical specifications of this sand, as discussed by Haghi et al. (2016) [16] and Abdellaoui et al. (2018) [17].

The oxides geochemistry can offer valuable information about both the origin of the samples and the prevailing weather conditions. The chemical maturity index (CMI), determined by the ratio of SiO_2 to Al_2O_3 abundance in the studied sand samples, falls within the range of 33 to 51, indicating the significant chemical maturity of the analyzed samples.

According to the binary change diagram of SiO_2 versus $Al_2O_3 + K_2O + Na_2O$ [18], we also found that all sand samples were formed under semi-arid/arid conditions. However, lower K_2O and Na_2O contents indicate lower feldspar concentration. In addition, we also confirmed that Fe_2O_3 + MgO ≤ 0.8% and $Al_2O_3/SiO_2 \leq 0.3$ in all samples, which indicates that they are related to passive continental margins according to the structural map of Bhatia (1983)[19].

The chemical index of alteration (CIA) and the chemical index of weathering (CIW) stand as the prevailing indices for evaluating the extent and duration of weathering in deposits. CIA is calculated using the formula $[Al_2O_3 \times 100/ (Al_2O_3 + Na_2O + CaO + K_2O)]$ [20], while CIW is determined by $[Al_2O_3 \times 100/ (Al_2O_3 + CaO + Na_2O)]$. As depicted in Table 1, the CAI and CIW values derived from the sand samples indicate a moderate to high degree of chemical weathering and corresponding environmental conditions [20].

3.2. X-ray Diffraction method (XRD)

Figure 3 displays the X-ray patterns of sand samples S1and S2 form the Bier El Ater and Engoussa area. These diffractograms confirms that all the samples of sand comprise mainly α-quartz (SiO_2) phase and a less quantity of calcite ($CaCO_3$) and gypsum ($CaSO_2$; $2H_2O$). The mineral identification was carried out by the X'Pert HighScore program and by using the JCPDS cards. The following diffractions are observed at 2θ angles values : 21.126°, 26.733°, 36,767° and 40.387°

corresponding respectively to the crystalline planes (100), (101), (110) and (111) of SiO_2 (α-quartz) hexagonal crystal structure under the space group P3221 (154), which is in agreement with JCPDS card N°00-046-1045 in the white sand (S1). As well as Engoussa sand dunes samples (S2) are characterized by diffraction peaks at 2θ: 20.827°, 26.607°, 36.489°, 39.429°, 40.234°, 42.384°, 45.728°, 54.803° and 55.277° for the crystalline planes (100), (011), (110), (102), (111), (200), (201), (022) and (013) respectively. These findings provide confirmation of the presence of quartz, as detailed in reference [21].

Calcium carbonate ($CaCO_3$) phase in S1 samples are observed at 2θ equal 42.962°(202) rhombohedral crystal structure with space group R-3c (167) according to the JCPDS card N° 01-083-1762 [22] and Gypsum phase ($CaSO_4$,$2H_2O$) are distinguished by values of 2θ angles : 50.381°(-262), 50.674°(-321) for S2 and 2θ = 50.317° (-262) crystalline plane in monoclinic structure space group I2/c as indicate the JCPDS card N° 01-074-1905 at S1 samples [23].

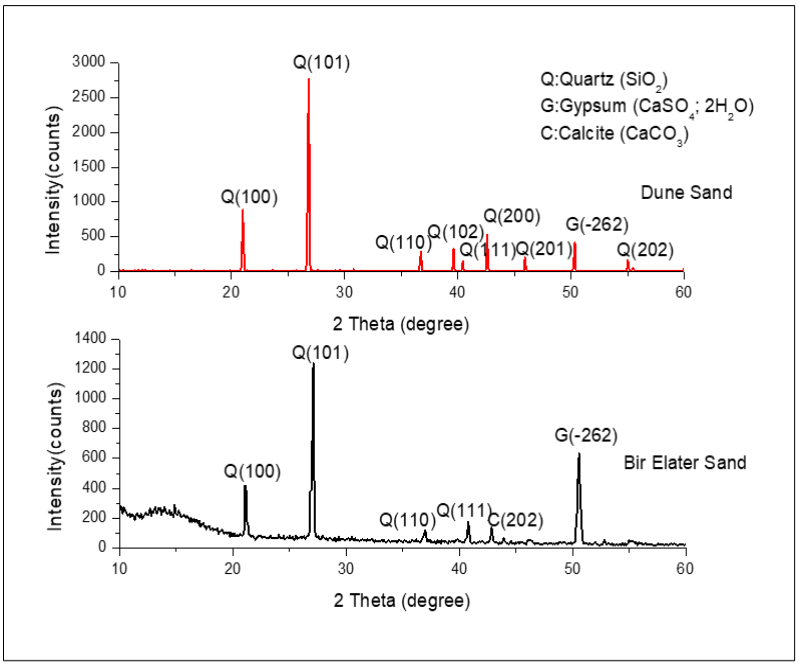

Fig. 2. XRD spectra of studied samples.

The shift observed in the positions of the peaks is probably due to the crystalline defects (shear planes, dislocations, and vacancies), which were may be caused by the initial formation. Further, the existence of impurities in the crystal lattice creates additional defects, affecting the crystal size and, therefore, the d spacing between lattice planes.

3.3. Fourier transformation infrared spectroscopy method (FTIR)

The FTIR spectra for the studied sand samples (S1 and S2) are presented in Fig. 3. It shows the characteristic bands of α-quartz phase at 459, 692, 779, 795, 1080, 1170, and 1878 cm^{-1}; these

bands are assigned to symmetric stretching and bending vibration of Si–O and Si–O–Si bond [24-25].

The vibration bands observed at 710, 1467, 1543, 1711, and 1742cm^{-1} confirm the presence of calcium carbonate [28-29]; that are attributed to the C=O stretching mode, the asymmetric stretching (ν3), out-of-plane bending (ν2) and in-plane bending (ν4) modes of (CO_3) [30]. The peaks observed at 2849and 2925cm^{-1} signifying the organic impurities [31]; they are assigned to C–H bond vibration [32]. The broad band at 3426 cm^{-1} can be related to water O–H bending and /or silanol groups stretching [12]. The FTIR spectrum of S2 samples shows band vibration at 3547 cm^{-1} characteristic of the gypsum [32] and a band at 3407 cm^{-1} characteristic of O-H vibration indict the presence of water H_2O.

3.4. SEM morphological analysis

Figure 8 displays the surface micrograph of sand samples. White sand granules from Bier El Ater show characteristics of subangular, rounded, well-rounded, and irregular grains.

In contrast, the dune sand sample obtained from Engoussa displays subangular shapes and low sphericity. Earlier investigations have revealed that the spherical configuration of granules tends to rise proportionally with the distance sediments travel from their initial source to sedimentation sites. Moreover, an observation was made indicating that windblown sediments tend to possess a more spherical shape compared to waterborne sediments [33].

Table. 1. Chemical analysis of our samples by XRF analysis.

Sample	SiO_2 (%)	CaO (%)	Al_2O_3 (%)	Fe_2O_3 (%)	K_2O (%)	MgO (%)	Na_2O (%)	Cl (%)
S1	92.05	2.27	2.77	2.14	0.42	0.26	0.07	0.02
S2	88.03	8.89	1.72	0.36	0.34	0.42	0.25	-

Sample	SiO_2/Al_2O_3	Fe_2O_3 + MgO (%)	Al_2O_3/SiO_2	$Al2O_3$ + Na_2O + K_2O (%)	CIA	CIW
S1	33.23	2.4	0.03	3.26	42.41	42.41
S2	51.18	0.78	0.02	2.31	15.12	15.12

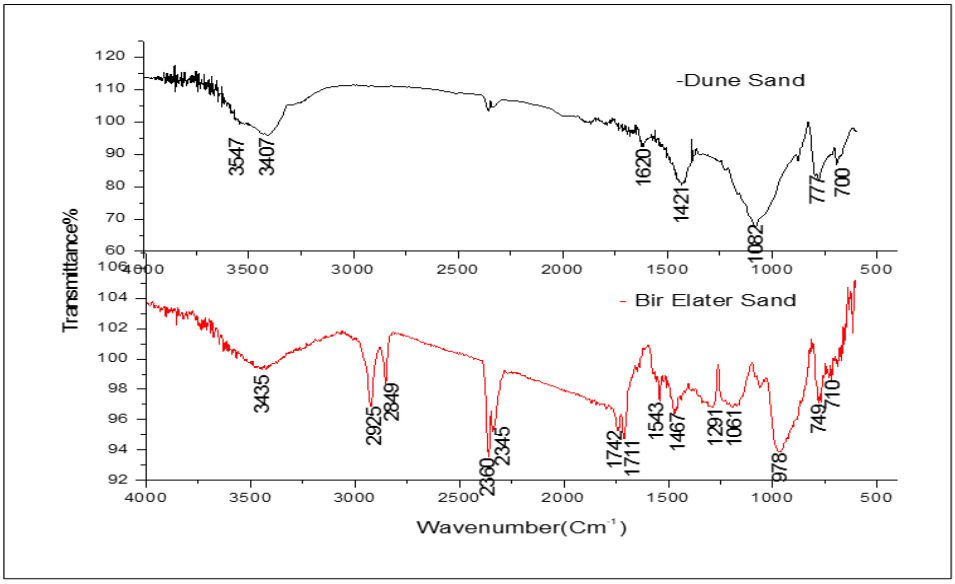

Fig. 3. FTIR absorption spectrums of studied samples.

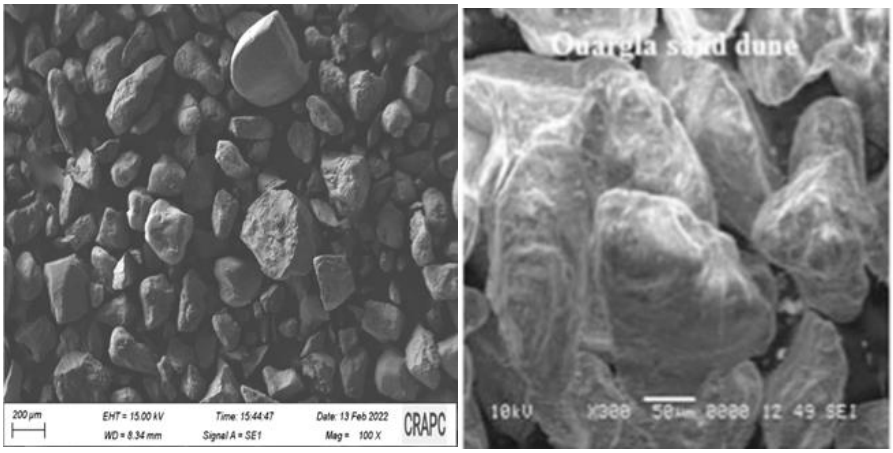

Fig. 4. Scanning electron micrographs of sand samples; (S1) the white sand, (S2) the dune sand.

3.5. Grain size distribution

The particle size distribution of sand a vital role as a textural parameter in assessing its appropriateness for diverse applications [27, 34-35]. This parameter offers insights into the transportation, sorting, and deposition conditions of the examined sand [6, 36]. The granulometric curves for the S1 and S2 samples can be found in Figure 3.

For white sand, the range of grain size values can be distinguished from 88.583 µm to 1754.63 µm, classified as sand (99%) and from 2009.687 µm to 2301.841 µm, identified as gravel (Fig. 5). In comparison, the Engoussa dunes sand have sands ranging from 200 µm to 1754.63 µm (90%).

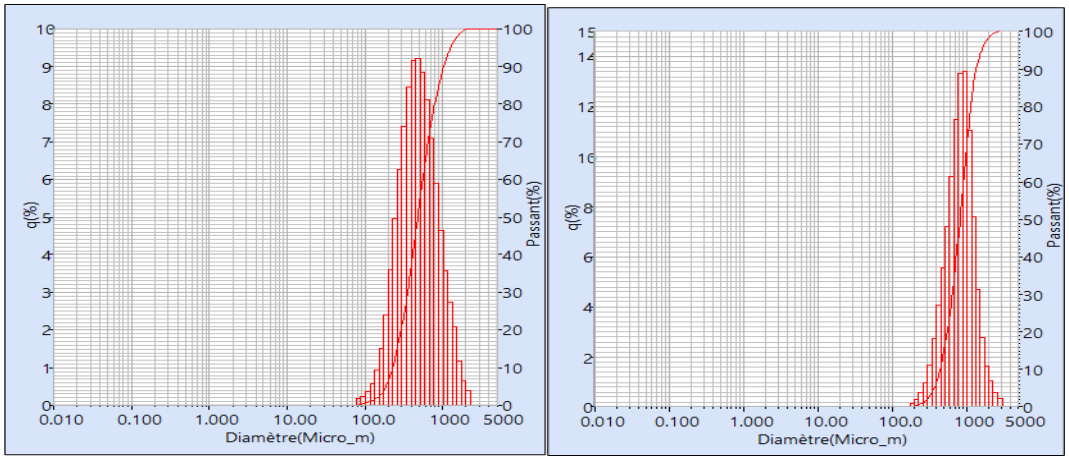

Fig. 5. Grain size distribution of sand samples; (S1) the white sand, (S2) the dunes sand.

4. Conclusion

Comprehensive examinations of the physicochemical, mineralogical, and morphological properties of Bier El Ater and Engoussa sand were conducted by FTIR, XRF, XRD, SEM and granulometric analysis.

The outcomes of our study revealed that chemical analyses conducted by XRF and FTIR indicated high silica content (92.05%) with minor impurities such as carbonates and other oxides including Al_2O_3, Fe_2O_3, Na_2O, and MgO. This finding was corroborated by the XRD technique.

The granulometric analysis (LA-960) revealed that white sand size distribution is dominated by grains ranging from 88.583 µm to 1754.63 µm in diameter. Engoussa dune sand exhibited particle sizes ranging from 200 µm to 1754.63 µm.

The sand samples from these areas showed subangular shapes and low sphericity for the dune sand of Engoussa areas, whereas the white sand of the Bier El Ater region exhibited an subangular, rounded, well-rounded, and irregular morphology.

The identified physicochemical attributes indicate that these sands are suitable for concrete, foundry, ceramic industry, as well as for purposes like solar energy storage and glass manufacturing. As a result, these versatile applications encourage the utilization and investigation of the sand dune as a local georesource, directly contributing to the sustainable development of the geomaterial sector in Algeria.

References

[1] S. K. Kirthika, S. K. Singh, A. Chourasia, Alternative fine aggregates in production of sustainable concrete-A review, Journal of cleaner production, 268, 122089. 2020 https://doi.org/10.1016/j.jclepro.2020.122089

[2] M. G. Elipe, S. López-Querol, Aeolian sands: Characterization, options of improvement and possible employment in construction–The State-of-the-art, Construction and Building Materials, 73, 728-739. 2014 https://doi.org/10.1016/j.conbuildmat.2014.10.008

[3] S. Lopez-Querol, J. Arias-Trujillo, G. E. Maria, A. Matias-Sanchez, B. Cantero, Improvement of the bearing capacity of confined and unconfined cement-stabilized aeolian sand. Construction and Building Materials, 153, 374-384, 2017 https://doi.org/10.1016/j.conbuildmat.2017.07.124

[4] K. Ganesan, V. Kanagarajan, J. R. J. Dominic, Influence of marine sand as fine aggregate on mechanical and durability properties of cement mortar and concrete, Materials Research Express, 9(3), 035504, 2022https://doi.org/10.1088/2053-1591/ac5f88

[5] E. S. S. Abu Seif, Geotechnical approach to evaluate natural fine aggregates concrete strength, Sohag, Governorate, Upper Egypt, Arabian Journal of Geosciences, 8(9), 7565- 7575, 2015. https://doi.org/10.1007/s12517-014-1705-3

[6] C. Li, Z. Zhang, Q. Chen, S. Dong, X. Yu, Q. Yu, Provenance of eolian sands in the Ulan Buh Desert, north western China, revealed by heavy mineral assemblages, Catena, 193, 104624,2020. https://doi.org/10.1016/j.catena.2020.104624

[7] S. Lopez-Querol, J. Arias-Trujillo, G. E. Maria, A. Matias-Sanchez, B. Cantero, Improvement of the bearing capacity of confined and unconfined cement-stabilized aeolian sand. Construction and Building Materials, 153, 374-384, 2017. https://doi.org/10.1016/j.conbuildmat.2017.07.124

[8] S.Amri, M. Akchiche, A. Bennabi, R. Hamzaoui, Geotechnical and mineralogical properties of treated clayey soil with dune sand. Journal of African Earth Sciences, 152, 140- 150, 2019. https://doi.org/10.1016/j.jafrearsci.2019.01.010

[9] A. Moulay-Ali, M. Abdeldjalil, H. Khelafi, An experimental study on the optimal compositions of ordinary concrete based on corrected dune sand—Case of granular range of 25 mm, Case Studies in Construction Materials, 14, e00521,2021.

[10] F. J. Luo, L. He, Z. Pan, W. H. Duan, X. L.Zhao, F. Collins, Effect of very fine particles on workability and strength of concrete made with dune sand. Construction and Building Materials, 47, 131-137, 2013. https://doi.org/10.1016/j.conbuildmat.2013.05.005

[11] A. Smaida, S. Haddadi, A. Nechnech, Improvement of the mechanical performance of dune sand for using in flexible pavements. Construction and Building Materials, 208, 464- 471, 2019. https://doi.org/10.1016/j.conbuildmat.2019.03.041

[12] N. Meftah, A. Hani, A. Merdas, C.Sadik, A. Sdiri, A holistic approach towards characterizing the El-Oued siliceous sand (eastern Algeria) for potential industrial applications. Arabian Journal of Geosciences, 14, 1-14, 2021. https://doi.org/10.1007/s12517-021- 08591-1

[13] N. Meftah, M. S. Mahboub, Spectroscopic characterizations of sand dunes minerals of El-Oued (Northeast Algerian Sahara) by FTIR, XRF and XRD analyses,Silicon, 12(1), 147-153,2020. https://doi.org/10.1007/s12633-019-00109-5

[14] Blanc N, Sand spreads its science, West Science Magazine, 2011, July, 12-13

[15] K. N. Jallad, C. Espada-Jallad, Spectroscopic characterization of geological materials from the United Arab Emirates. Arab J Geosci 1(2):119–127,2008.

[16] J. Fontaine, In Annales de géographie. Armand Colin, 4, 437-448, 2005.

[17] L.J. Suttner, P.K. Dutta, Alluvial sandstone composition and paleoclimate; I, Framework mineralogy, J Sediment Res 56(3):329– 345,1986. https://doi.org/10.1306/212F8909-2B24-11D7-8648000102 C1865D

[18] M. R. Bhatia, Plate tectonics and geochemical composition of sandstones, The Journal of Geology 91(6):611–627, 1983. https://www. jstor.org/stable/30064711

[19] H. W. Nesbitt, G. M. Young, Early Proterozoic climates and plate motions inferred from major element chemistry of lutites, Nature 299:715–717, 1982. https://doi.org/10.1038/299715a0

[20] C. M. Fedo, H. W. Nesbitt, G. M. Young, Unravelling the effects of potassium metasomatism in sedimentary rocks and paleosols, with implications for paleoweathering conditions and provenance, Geology23:921–924,1995.https://doi.org/10.1130/0091-7613(1995)023%3c0921:UTEOPM%3e2.3.CO;2

[21] A. Kern, W. Eysel, Mineralogisch-Petrograph, Inst., Univ. Heidelberg, Germany., ICDD Grant-in-Aid, (1993)

[22] H. Effenberger, K. Mereiter, J. Zemann, Z. Kristallogr. , 156, 233, (1981)

[23] M. Atoji, R.E. Rundle, J. Chem. Phys, 29, 1306, (1958)

[24] M.L. Mechri, S. Chihi, N. Mahdadi, S. Beddiaf, Diagnosis of the heating effect on the electrical resistivity of Ouargla (Algeria) dunes sand using XRD patterns and FTIR spectra. J African Earth Sci 125:18–26, 2017. https://doi.org/10.1016/j.jafrearsci.2016.10.007

[25] R.S. Kumar, P. Rajkumar, Infrared Physics & Technology Characterization of minerals in air dust particles in the state of Tamilnadu. India through FTIR, XRD and SEM Analyses 67:30–41, 2020. https://doi.org/10.1016/j.infrared.2014.06.002

[26] F. B. Reig, J. V. G. Adelantado, M. C. M. Moreno, FTIR quantitative analysis of calcium carbonate (calcite) and silica (quartz) mixtures using the constant ratio method, Application to geological samples, Talanta 58: 811-821, 2002.

[27] N. J. Saleh, R. I. Ibrahim, A. D. Salman, Characterization of nanosilicaprepared from local silica sand and its application in cementmortar using optimization technique. Adv Powder Technol26:1123–1133, 2015. https:// doi.org/ 10.1016/j. apt. 2015. 05. 008

[28] A. A. Flemming, B. Ljerka, infrared spectra of amorphous and crystalline CalciumCarbonate. Acta Chem. Scand 45: 1018-1024, 1991.

[29] A. Sdiri, T. Higashi, T. Hatta, Mineralogical and spectroscopic characterization, and potential environmental use of limestone from the Abiod formation, Tunisia. Environ Earth Sci 61:1275–1287, 2010. https://doi.org/10.1007/s12665-010-0450-5

[30] Y. Yanshan, Y. Huixia, W. Zihua, Q. Caiwen, T. Hong, Z. Wei, H. Zhangmao, F. Leihua, Characterization of coals and coal ashes with high Si content using combined second-derivative infrared spectroscopy and Raman spectroscopy, Crystals, 2019. https://doi.org/10.3390/cryst9100513

[31] B. Hasan, A. Sedat, Ö. E. Serhan, G. Hale, N. C. S Emine, Quantification of CaCO3–CaSO30.5H2O–CaSO42H2O mixtures by FTIR analysis and its ANN model. Mater Lett 85:723–726, 2004. https://doi.org/10. 1016/j.matlet.2003.07.008

[32] K. Kihara, X-ray study of the temperature dependence of the quartz structure. Eur J Mineral 2:63–77, 1990.

[33] A. S. Ahmad, M. A. Ahmad, Introduction to sedimentology. The Anglo - Egyptian library, Cairo, P76–79 (in Arabic), 2007.

[34] M. Diago, A. C. Iniesta, A. Soum-Glaude, N. Calvet, Characterization of desert sand to be used as a high-temperature thermal energy storage medium in particle solar receiver technology. Appl Energy 216:402–413, 2018. https://doi.org/10.1016/j.apenergy.2018.02.106

[35] S. A. Osseni, M. Masseguin, E.V. Sagbo, Physico-chemical characterization of siliceous sands from Houéyogbé in Benin Republic (West Africa): potentialities of use in glass industry. SILICON 11:2015–2023, 2019. https://doi.org/10.1007/s12633-018-0022-y

[36] N. Lancaster, W.G. Nickling, N. C. McKenna, Particle sizeand sorting characteristics of sand in transport on the stossslopeof a small reversing dune.Geomorphol 43:233–242(2002) https:// doi.org/10. 1016/ S0169- 555X(01) 00135-0